

Laser-Driven Ion Acceleration in a Hybrid RPA-TNSA Regime

Contact *s.kar@qub.ac.uk*

D. Gwynne, S. Kar *, H. Ahmed, D. Doria, F. Hanton, M. Zepf, M. Borghesi

Centre for Plasma Physics, Queen's University Belfast, University Road, Belfast, BT7 1NN

M. Cherchez, M. Swantusch, O. Willi

Institut für Laser-und Plasmaphysik, Heinrich-Heine-Universität, Düsseldorf, Germany

J. Fernandez, J.A. Ruiz

Instituto de Fusion Nuclear UPM, Jose Gutierrez Abascal 2, E28006 Madrid, Spain

J.S. Green, D. Neely

Central Laser Facility, Rutherford Appleton Laboratory, Didcot, Oxfordshire, OX11 0QX

R.J Gray, D.A. MacLellan, P. McKenna

Department of Physics, SUPA, University of Strathclyde, Glasgow, G4 0NG

Z. Najmudin, M. Streeter

Blackett Laboratory, Imperial College London, London, SW7 2AZ

Introduction

Acceleration of energetic ion beams by ultra-intense laser interactions with thin foils is a subject which has recently received a great deal of attention from both theoretical and experimental points of views [1]. Laser-driven ion acceleration has the potential to be a cost effective and compact alternative to conventional accelerators for scientific, technological and healthcare applications [2]. Most of the experimental research carried out in this field to date is related to the so-called target normal sheath acceleration (TNSA) mechanism. In a number of experiments performed in the past, employing different laser-systems and under different interaction conditions, protons of several tens of MeV were produced from thin foils irradiated with high intensity pulses. However, the TNSA mechanism lacks prospective due to several unfavorable beam parameters, such as large divergence, exponential energy spectrum and slow ion energy scaling. By contrast, ion production by the radiation pressure of intense lasers has been predicted to be a promising route for accelerating large numbers of ions quasi-monoenergetically to the GeV/nucleon range in a more efficient manner [2,3].

In radiation pressure acceleration (RPA) mechanism, the ions are accelerated by directional momentum transfer from the laser to the target via the laser's ponderomotive force. The ponderomotive force acts as a snow-plough on the target front surface and launches a dense ion bunch into the target. In every laser cycle, the radiation pressure instantly pushes the electrons in the skin depth and sets up a strong accelerating field for the ions to promptly follow the electrons [3]. For a thick target, it appears as if a hole is bored through the target by the laser pulse, hence this is called the hole-boring (HB) regime of the RPA mechanism. If the target thickness is less than the product of the laser pulse duration and the hole-boring velocity, the ions will pile up at the target rear surface before the end of the laser pulse. As the thickness of the compressed layer becomes comparable to or less than the evanescence length of the ponderomotive force, the whole layer is cyclically accelerated with high efficiency for the rest of the duration of the laser pulse. This regime of acceleration of the compressed layer as a whole has been called the light-sail (LS) regime of the RPA mechanism. As predicted by several experimental and computational studies [2-6], the light-sail regime of RPA is particularly promising due to a favorable ion energy scaling

with the incident laser fluence [4–6], while producing ions with narrow energy spectra and significantly lower divergence compared to that typically produced by the TNSA mechanism.

The experimental results presented in this report show evidence of narrow band features in the ion spectra produced from ultrathin (10 nm) high Z foils irradiated by the intense VULCAN Petawatt laser. Peaks in the carbon (C^{6+}) spectra around of 12 MeV/nucleon are observed which is a two-fold increase in ion energy compared to what was obtained with thicker foils at the same laser facility [2,3]. A systematic scan over several laser and target parameters yields data which extends the quadratic ion energy scaling with the dimensionless scaling parameter for the RPA mechanism, in the previously reported results. One of the key findings of the campaign was the observation of similar ion energy even after the temporal stretching of the laser pulse by a factor of 5, which underpins the role of laser fluence, rather than laser intensity, in the RPA regime.

Experimental Arrangement

The experiment was conducted employing the Petawatt arm of the Vulcan laser system at the Rutherford Appleton Laboratory. A schematic of the experimental setup is shown in Figure 1. The laser energy on target and the pulse duration was varied from 100-250J and 1.0–5.2 ps respectively in order to conduct energy and pulse duration scans. The laser was focused onto the

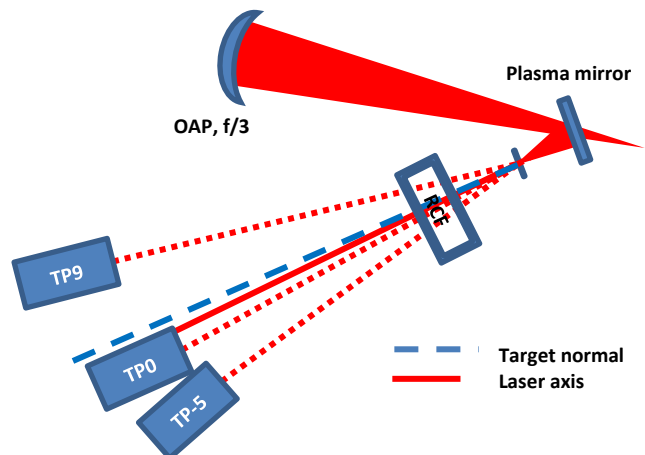


Figure 1: Schematic of the experimental setup.

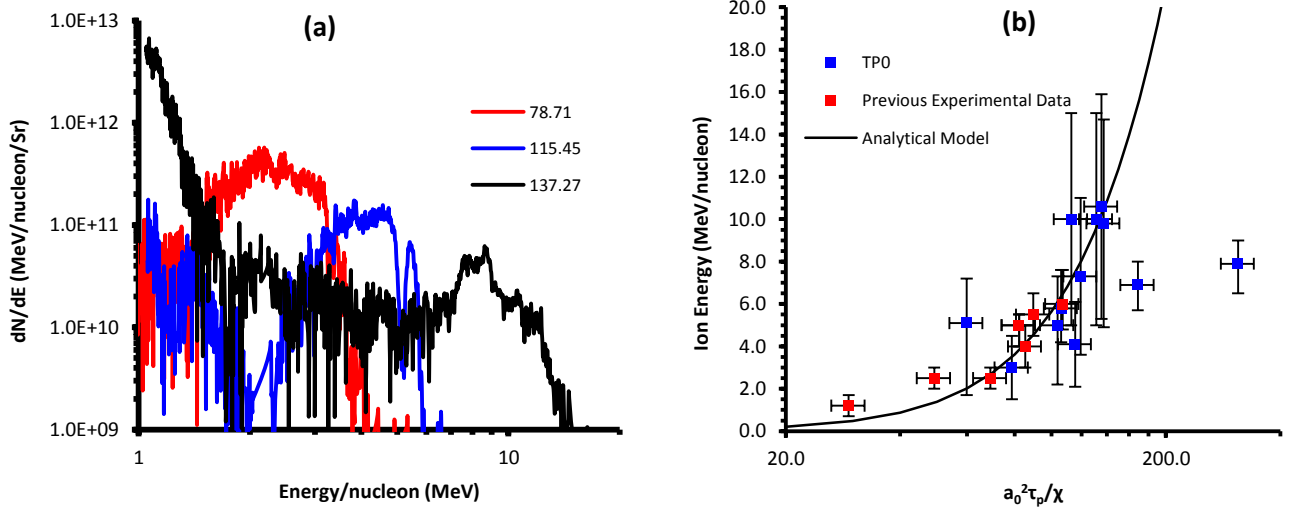


Figure 2: (a) The C^{6+} ion spectra of three different shots with three different values of $a_0^2\tau_p/\chi$, showing an increase in the peak energy with an increase in the value of $a_0^2\tau_p/\chi$. (b) Positions of the spectral peaks plotted as a function of $a_0^2\tau_p/\chi$ for TPO. The black line represents the ion energy estimated from the analytical model described in ref. [2] and the red squares represent the experimental data points reported in ref. [2]

target at normal incidence by a $f/3$ off-axis parabolic mirror, after being reflected from a plasma mirror. The laser focal spot on target was measured as ~ 5 microns FWHM by using a CW alignment laser, which was set with similar beam quality as the VULCAN laser. Depending on the incident energy and pulse duration, the peak intensity on target varied over the range $\approx 2 \times 10^{19}$ to $2 \times 10^{20} \text{ Wcm}^{-2}$. Targets of different thickness (10 nm – 100s of nm) and materials (Ag, Al, Au, Cu) were irradiated in order to conduct a target areal density scan. The multi-species ions produced during the irradiations were diagnosed by three high resolution Thomson Parabola (TP) Spectrometers [7] employed at $-5, 0$ and 9 degrees from the laser axis, as shown in Figure 1. The ion spectra were recorded by using BAS-TR image plates as detectors in the TPs. In order to obtain particle numbers from the image plate data, the image plates were cross-calibrated with CR39 nuclear track detectors for several ion species such as proton, carbon and high Z Au ions. Stacks of radiochromic film detectors were used closer to target in order to obtain the beam profile of accelerated protons from the interaction.

Results

Unlike the exponential ion spectra produced from micrometre thick foils by the TNSA mechanism, narrow band features in proton and heavier ion spectra were clearly observed from ultrathin (10s of nm) foil. Figure 2(a) shows typical carbon ion ($Z/A = 0.5$) spectra from three different shots, showing an increase in ion energy with increasing dimensionless fluence parameter, $a_0^2\tau_p/\chi$, where $a_0 = 0.85 \sqrt{I_0\lambda^2/10^{18} \text{ Wcm}^{-2}}$, $\tau_p = ct_p/\lambda$, $\chi = p'l/\lambda$, $p' = \rho/m_p n_c$, I_0 is the peak laser intensity (in Wcm^{-2}), λ is the laser wavelength ($1.054 \mu\text{m}$), t_p is the laser pulse duration (in ps), c is the speed of light in vacuum, l is the target thickness, ρ is the target density, m_p is the mass of a proton and n_c is the critical electron density ($1 \times 10^{21} \text{ cm}^{-3}$). One can see the pronounced narrow band spectral features, clearly separated from the lower energy components, which could be attributed to the RPA mechanism showing an onset of dominance over TNSA mechanism along the laser forward direction. Due to the strong electron heating during the high intensity interaction, TNSA mechanism is expected to coexist and most likely to play a role towards broadening of the spectral peaks as well as continuing acceleration of the lower energy ions even after the end of the laser pulse. Such a regime was referred to as a hybrid TNSA-RPA regime in ref. [8].

A plot of the ion energies at the spectral peaks observed for a number of shots by varying laser energy, target material and thickness is shown in Figure 2(b) as a function of the dimensionless fluence parameter. The peak energies were determined by taking the average value of the ion energies between the abrupt rise and sharp energy cut-off in the observed spectral modulations. As can be seen from the figure, the data points scale quadratically with the dimensionless fluence parameter, in a similar way as the data points obtained from the previous experimental campaign at the Vulcan petawatt facility reported in the ref. [2]. The solid black line represent the theoretical fit from the simple analytical model reported in the ref. [2], which demonstrates that the observed peaks and their scaling with the target and laser parameters is consistent with the expected ion energies in light-sail acceleration. While spectral peaks up to $\sim 6 \text{ MeV/nucleon}$ were obtained in ref. [2], an increase of nearly a factor of two in the spectral peak energy was obtained in the current experiment by employing thinner targets.

The dependence of ion energy with incident laser fluence is one of the key advantages of radiation pressure acceleration, as it allows deployment of ultra-thin targets without being concerned about possible damage by prepulses/ASE typically associated with high intensity laser pulses, or, the onset of relativistic transparency due to ultra-high intensities. While keeping target areal density and laser pulse duration constant, an increase in the laser intensity will in principle lead to an increase in ion energy. However, as soon as the laser intensity becomes high enough to trigger the onset of relativistic transparency, the efficiency of ion acceleration via RPA drops abruptly [2,5,6]. The condition for obtaining optimum ion energy while avoiding the onset of relativistic transparency is given as $a_0 = \pi(n_e/n_c)(l/\lambda)$ [5], which limits the minimum target areal density that can be deployed at a given laser intensity. The constraint on the maximum ion energy can be mitigated by increasing the laser fluence on target while keeping laser intensity low on the target, i.e. by increasing the laser pulse duration while increasing the laser energy on the target.

Figure 3 shows the experimental data obtained in the campaign for two different laser pulse durations. Even by changing the pulse duration by a factor of five, while keeping other parameters such as laser energy, focal spot size, target material and thickness constant, the data shows no significant change in ion spectral profiles and the energy of the spectral peaks. The three shots which have been shown in Figure 3 have the same

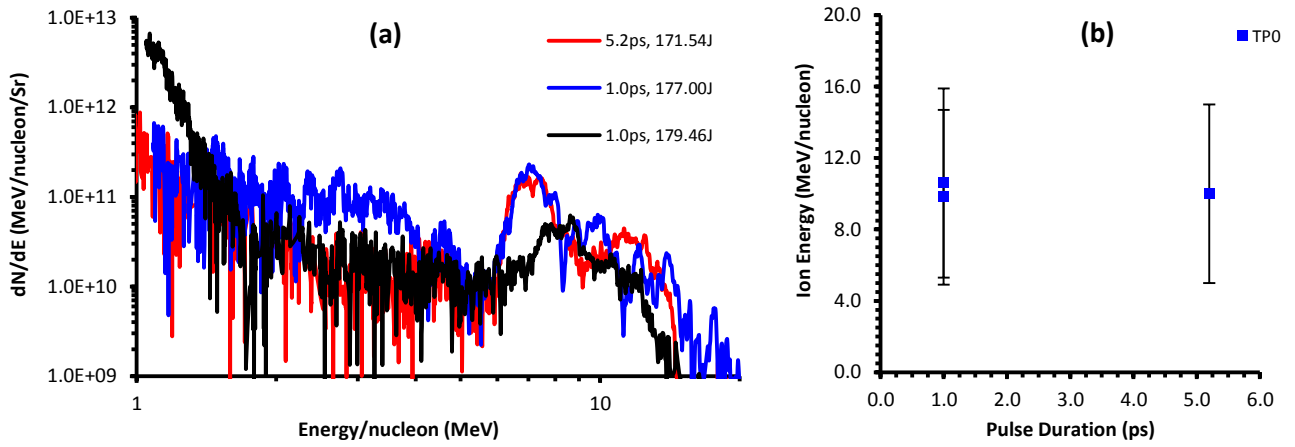


Figure 3: (a) C^{6+} spectra obtained from three shots on 10 nm Au targets of [energy on target (J), pulse duration (ps)] [171.54, 5.2], [177.00, 1.0] and [179.46, 1.0] shown in red, blue and black respectively. (b) Peak ion energy for each of the three shots for TPO plotted against pulse duration.

target thickness and material (10nm Au), roughly the same energy delivered to the target, but different pulse durations. Narrow band carbon peaks at ~ 10 MeV/nucleon are observed for the first time from laser foil interactions at intensities of $\sim 3 \times 10^{19}$ Wcm $^{-2}$, which is likely to be an indication of the role of radiation pressure acceleration during the interaction.

Shot	t_p (ps)	Energy (J)	Intensity (Wcm $^{-2}$)	Fluence (Jcm $^{-2}$)	$a_0^2 \tau_p / \chi$
1	5.2	171.54	2.68×10^{19}	3.95×10^8	131.21
2	1.0	177.00	1.44×10^{20}	4.07×10^8	135.39
3	1.0	179.46	1.46×10^{20}	4.13×10^8	137.27

Table 1: Summary of shot details shown in Fig. 3(a).

Conclusions

For the non-relativistic case, the ion energy obtained from the RPA mechanism is predicted to scale with the square of the dimensionless fluence parameter, $a_0^2 \tau_p / \chi$, as indicated by numerous analytical and numerical studies. It is therefore suggested that the ion energy can be enhanced by increasing the fluence of the laser and/or reducing the target areal density. While recent experimental data agrees with the same scaling reported by the previous experiment carried out at the same laser facility, there has been a successful increase in the ion energy achieved by employing thinner targets. At the same time, the dependence of ion energy on laser fluence was experimentally verified owing to the observation of similar ion energy while increasing the laser pulse duration by a factor of 5.

Acknowledgements

The authors acknowledge funding from EPSRC [EP/J002550/1-Career Acceleration Fellowship held by S. Kar, EP/L002221/1, EP/E035728/1, EP/K022415/1, EP/J003832/1, and EP/J500094/1], Laserlab Europe (EC-GA 284464), projects ELI (Grant No. CZ.1.05/1.1.00/483/02.0061) and OPVK 3 (Grant No. CZ.1.07/2.3.00/20.0279). Authors also acknowledge the support of the mechanical engineering staff of the Central Laser Facility, STFC, UK.

References

- [1] M. Borghesi, A. Mackinnon, D. Campbell, D. Hicks, S. Kar, P. Patel, D. Price, L. Romagnani, A. Schiavi, and O. Willi, Phys. Rev. Lett. **92**, 055003 (2004).
- [2] S. Kar, K. Kakolee, B. Qiao, a. Macchi, M. Cerchez, D. Doria, M. Geissler, P. McKenna, D. Neely, J. Osterholz, R.

Prasad, K. Quinn, B. Ramakrishna, G. Sarri, O. Willi, X. Yuan, M. Zepf, and M. Borghesi, Phys. Rev. Lett. **109**, 185006 (2012).

- [3] K. F. Kakolee, S. Kar, D. Doria, B. Qiao, M. Geissler, B. Ramakrishna, G. Sarri, K. Quinn, M. Zepf, and M. Borghesi, Cent. Laser Facil. Annu. Rep. 2010-2011 (2011).
- [4] A. Macchi, S. Veghini, and F. Pegoraro, Phys. Rev. Lett. **103**, 085003 (2009).
- [5] A. Macchi, S. Veghini, T. V Liseykina, and F. Pegoraro, New J. Phys. **12**, 045013 (2010).
- [6] A. P. L. Robinson, M. Zepf, S. Kar, R. G. Evans, and C. Bellei, New J. Phys. **10**, 013021 (2008).
- [7] D. Gwynne, S. Kar, D. Doria, H. Ahmed, M. Cerchez, J. Fernandez, R. J. Gray, J. S. Green, F. Hanton, D. a MacLellan, P. McKenna, Z. Najmudin, D. Neely, J. a Ruiz, a Schiavi, M. Streeter, M. Swantusch, O. Willi, M. Zepf, and M. Borghesi, Rev. Sci. Instrum. **85**, 033304 (2014).
- [8] B. Qiao, S. Kar, M. Geissler, P. Gibbon, M. Zepf, and M. Borghesi, Phys. Rev. Lett. **108**, 115002 (2012).